Biochemical Journal Immediate Publication. Published on 09 Jun 2011 as manuscript BJ20101316

Altering the stability of the Cdc8 overlap region modulates the ability of this tropomyosin to bind cooperatively to actin and regulate myosin.

Daniel A. East[†], Duncan Sousa[‡], Stephen R. Martin[§], Thomas A. Edwards[¶], William Lehman[‡] and Daniel P. Mulvihill[†,*]

[†] School of Biosciences, University of Kent, Canterbury, Kent, CT2 7NJ, UK.

[‡] Department of Physiology and Biophysics, Boston University, School of Medicine, Boston, MA 02118, USA.

[§] Division of Physical Biochemistry, MRC National Institute for Medical Research, The Ridgeway, Mill Hill, London NW7 1AA, UK.

[¶] Astbury Centre for Structural Molecular Biology, University of Leeds, Leeds LS2 9JT, UK

* Author for correspondence (e-mail: d.p.mulvihill@kent.ac.uk).

Key words: *Schizosaccharomyces pombe*, Tropomyosin, Cdc8, acetylation, coiled-coil, fission yeast.

Abstract

Tropomyosin (Tm) is an evolutionarily conserved α-helical coiled-coil protein, dimers of which form end-to-end polymers capable of associating with and stabilising actin-filaments and regulate myosin function. The fission yeast, *Schizosaccharomyces pombe*, possesses a single essential Tm, Cdc8, which can be acetylated on its amino terminal methionine to increase its affinity for actin and enhance its ability to regulate myosin function. We have designed and generated a number of novel Cdc8 mutant proteins with amino terminal substitutions to explore how stability of the Cdc8-polymer overlap region affects the regulatory function of this Tm. By correlating the stability of each protein, its propensity to form stable polymers, its ability to associate with actin and to regulate myosin, we have shown the stability of the amino terminal of the Cdc8 α-helix is crucial for Tm function. In addition we have identified a novel Cdc8 mutant with increased amino-terminal stability, dimers of which are capable of forming Tm-polymers significantly longer than the wild-type protein. This protein had a reduced affinity for actin with respect to wild type, and was unable to regulate actomyosin interactions. The data presented here are consistent with acetylation providing a mechanism for modulating the formation and stability of Cdc8 polymers within the fission yeast cell. The data also provide evidence for a mechanism in which Tm dimers form end-to-end polymers on the actin-filament, consistent with a cooperative model for Tm binding to actin.

Introduction

Tropomyosin (Tm) is an evolutionarily conserved dimeric α-helical coiled coil protein that associates with actin filaments. Tm dimers associate on actin, in an end-to-end fashion to create an unbroken polymer that stabilises actin filaments, as well as regulate actomyosin interactions and actin filament dynamics in both muscle and non-muscle cells. For smooth and skeletal muscle tropomyosin, acetylation of the amino terminus is required for strong binding to actin [1, 2] and thus to regulate myosin interaction. Acetylation allows the amino terminus of Tm to adopt a fully coiled-coil conformation [3-5] and 'slot' into splayed carboxyl terminus of another Tm dimer [4, 6] forming a strong end-to-end interaction. The first 2-3 amino terminal residues of unacetylated Tms, such as those recombinantly expressed in bacteria, are non-helical and as such form weaker end-to-end interactions and have reduced affinity for actin.

Dimeric α-helical coiled coil proteins have a heptad pseudo-repeating sequence periodicity (residue positions are termed *a* to *g* – Figure 1A). Lateral interactions between residues of adjacent proteins (hydrophobic interactions between residues in the *a* and *d* positions and ionic interactions between residues in *e* and *g* positions) stabilise the coiled-coil structure [3, 7].

The mechanism by which Tm associates with actin is the subject of an ongoing debate. One model suggests the existence of specific actin interacting zones along the Tm filament which together provide sufficient electrostatic attraction with the actin polymer to promote binding [8, 9]. A second model argues the intrinsic curvature of the Tm dimer facilitates its interaction with the actin filament in a cooperative mechanism, recently termed the 'Gestalt' model of Tm binding (for review see [10]). Due to the weak affinity of individual Tm dimers for actin (> 20 μM), Tm must associate end-to-end to form a continuous polymer along the actin filament. The amino and carboxyl termini are essential for end-to-end interaction and therefore actin affinity [11]. Studies with endogenous and recombinant Tms have established that modifications to the amino and carboxyl termini alter end-to-end interactions, actin affinity [1, 12] and interaction with myosin [13] along the actin filament .

The fission yeast *Schizosaccharomyces pombe* is a model organism amendable to cell, molecular, biochemical and genetical approaches. It has a single tropomyosin encoded by the *cdc8*$^{+}$ gene which is essential for cell viability [14]. Previous work has shown that like muscle Tm, acetylation of Cdc8 is required for strong actin binding and myosin regulation [15] but is not essential for the viability of the fission yeast cell [16].

In this study we use a series of novel Cdc8 amino terminal mutants to explore how stability of the Cdc8 overlap region affects the physical properties and regulatory function of this Tm. By correlating the stability of each protein and its propensity to form polymers with its ability to associate with actin and regulate myosin, it has been possible to establish that the stability of the Tm-polymer is crucial for its function. These data suggest a mechanism by which acetylation regulates the length of the Tm-polymers to permit efficient association with actin-filaments and thereby regulate myosin, consistent with a cooperative binding model of Tm binding to actin.

EXPERIMENTAL

Yeast cell culture and strains

The yeast strains used in the study are wt (DMY244) h^+ *his2-d1 ura4.d18 leu1.32*; *cdc8-110* (DMY333) h^+ *cdc8-110 his2-d1 ura4.d18 leu1.32*. Cell culture and maintenance were carried out according to [17] using minimal medium (EMM2) supplemented with appropriate amino acids.

Molecular Modelling

The model presented in Figure 1C & D was generated using the following procedure: The *S. pombe* Cdc8 and chicken Tm alpha1 were aligned such that the N and C termini were each aligned according to the heptad repeats. The structure of the tropomyosin overlap complex from chicken smooth muscle (PDB code 3MTU [4]) was then mutated to the Cdc8 sequence using this alignment. Figure 1C & D was generated using PyMol (The PyMOL Molecular Graphics System, Version 1.3, Schrödinger, LLC).

Molecular Biology and Protein Purification

cdc8 mutants were generated by site directed mutagenesis using pJC20*cdc8*$^+$ template [15] with appropriate oligonucleotides (Table 1). Each mutant was sequenced and also cloned into the fission yeast plasmid pREP41. Cdc8 proteins were purified as described previously [15] and concentrations were determined using a 280nm extinction coefficient of 2980cm^{-1}.

ATPase assays

Reactions were prepared in ATPase buffer (10 mM MOPS, 30mM NaCl, 5 mM $MgCl_2$ pH 7) containing 150 µM phosphoenolpyruvate (PEP), 150 µM NADH, 150 µM ATP, 10µl of pyruvate kinase/lactate dehydrogenase enzyme mix (Sigma-Aldrich). Varying concentrations of rabbit myosin II sub-fragment 1 (S1) were then added to the 1ml plastic cuvettes (Sarstedt) and allowed to equilibrate for 1 minute at 25 ºC. Actin or actin saturated with Cdc8 proteins (30 minute pre-incubations of actin and Cdc8 were performed at 25 ºC) was added to the reactions and mixed with a plastic stir-rod. Total reaction volume was 500 µl. Absorbance at 340 nm was monitored using a UV/Visible spectrophotometer (Varian Carey 50 Bio) connected to a PC and rates calculated from the slope of the curve.

Cosedimentation and quantitative electrophoresis

Cosedimentation assays were performed at 25 ºC by mixing 10 µM actin with increasing concentrations of Cdc8 in cosedimentation buffer (20 mM MOPS, 100 mM KCl, 5 mM $MgCl_2$, pH 7.0) in an total of 100 µl. Reactions were incubated for 30 mins. Actin along with any bound tropomyosin was pelleted by centrifugation at 100,000 RPM for 20 minutes (Beckman Instruments TLA-100.1). Equal samples of pellet and supernatant were separated by SDS-PAGE. Gels were scanned using an Epson perfection 1640SU scanner with a transparency adaptor attached to a PC and analysis was performed using Scion Image software (Scion Corp., Frederick, MD).

Viscosity analysis: A Cannon-Manning semi-microviscometer was used to determine the viscosity of 20 µM Cdc8 samples at 20 ± 1 ºC in 1 ml of viscometry buffer (20 mM MOPS, 5 mM $MgCl_2$ pH 7.0). NaCl concentration was increased from 0 to 250 mM. Kinematic viscosity was calculated using the manufacturer's predetermined microviscometer kinematic viscosity

constant and the average efflux time, calculated from 5 observations per sample at each NaCl concentration.

Circular Dichroism

Circular dichroism measurements were made in 1 mm quartz cuvettes using a Jasco 715 spectropolarimeter. Cdc8 proteins were diluted in CD buffer (10 mM Potassium phosphate, 500 mM NaCl, 5 mM $MgCl_2$ pH 7.0) to a concentration of 0.4 mg/ml. Thermal unfolding data were obtained by monitoring the CD signal at 222 nm with a heating rate of 1 deg/min. CD data are presented as differential absorption (ΔA) or mean residue CD extinction coefficient ($\Delta\varepsilon_{mrw}$) CD data were analyzed as a simple two-state equilibrium between the folded dimer (F_2) and the unfolded monomer (U).

$$F_2 \overset{K}{\rightleftharpoons} 2U$$

The unfolding constant is defined as $K = [U]^2/[F_2]$ and the total concentration of protein (P_0) is given by $P_0 = [U] + 2[F_2]$. The fraction of unfolded monomer present can be defined as $F_U = [U]/P_0$.
Therefore:

$$F_U = \frac{-K + \sqrt{K^2 + 8KP_0}}{4P_0} \qquad (1)$$

F_U at the mid-point of the unfolding transition (T_m) is equal to 0.5 by definition.

Therefore:

$K_{Tm} = P_0$ and $\Delta G_{Tm} = \Delta H_{Tm} - T_m\Delta S_{Tm} = -RT_mLn(P_0)$. If one assumes that $\Delta C_p \sim 0$ then for all temperatures one has $\Delta H_T = \Delta H_{Tm}$ and $\Delta S_T = \Delta H_{Tm}/T_m + RLn(P_0)$.

Therefore:

$$K_T = P_0 \exp\left(\frac{\Delta H_{T_m}}{R}\left(\frac{1}{T_m} - \frac{1}{T}\right)\right) \qquad (2)$$

CD data collected as a function of temperature were analyzed using the following equation:

$$CD_T = (a+bT)(1-F_u) + (c+dT)F_u$$

Where a,c and b,d are the intercepts and slopes of the of the pre- (a,b) and post-transition (c,d) regions and F_u is obtained from equation (1) with K_T from equation (2).

EM rotary shadowing:

Tm samples were diluted to 1.0 µM in a solution consisting of 5 mM Tris (pH 7.0), 5 mM KCl, 5 mM $MgCl_2$ and including 30 % glycerol were sprayed onto freshly cleaved mica. Platinum evaporation and rotary shadowing was carried out as in [18]. Electron microscopy was carried out on the shadowed molecules using a Philips CM120 electron microscope (FEI, Hillsboro, OR) at

120 kV and images digitized at 28,000 times magnification with a 2Kx2K F224HD slow scan CCD camera (TVIPS, Gauting, Germany). The recorded images of tropomyosin were then skeletonized following manual selection of 0.5 x 0.5 nm points every 4 to 5 nm along the center of the protein's longitudinal axis [19, 20]. The persistence length, ξ, was calculated, using the tangent angle correlation method, after determining θ (the deviation angles along tropomyosin molecules and polymers from an idealized straight rod) for segment lengths between 50 and 400 nm. Algorithms specifically tailored to determine ξ and θ were developed previously [19, 20]. Plots relating the inverse slope of <ln(cos θ)> to the segment length yields the persistence length values, where the factor of two in $\langle \cos(\dot{e}(s)) \rangle = e^{-s/2\dot{i}}$ accounts for the two dimensionality of the images [19, 20].

RESULTS

We wished to examine the role Cdc8 end-to-end interactions played in regulating the ability of this Tm to associate with actin and regulate myosin activity. To do this we designed mutations within the Cdc8 molecule that have the potential to disrupt the overlap region without affecting the integrity of the Cdc8 dimer. The carboxyl termini of different Tms diverge significantly, making it not only difficult to identify residues that may be key in protein-protein interactions, but also challenging for correlating findings with Tms from other cell types. In contrast the amino termini of Tm proteins are highly conserved between yeast and metazoan species (Figure 1B) and it has been shown that small changes to this region can have a significant impact upon the function of this protein [21].

Using homology alignments (Figure 1B) and molecular modelling of the Cdc8 overlap region (Figure 1C) we attempted to identify charged residues within the amino terminal region that have the potential to form electrostatic interactions with actin or the carboxyl terminus of an adjacent Cdc8 dimer, but were unlikely to affect dimer stability. Using this method we identified 2 conserved acidic residues (D2 & E6) within the Cdc8 amino terminus that sit in the *b* and *f* heptad positions of the coiled-coil (Figure 1A) and are therefore unlikely to disrupt the coiled-coil dimer. We also mutated a conserved acidic residue in a comparable b position (D16) to examine the effect charged residues predicted to lie outside of the overlap region had upon dimer stability or end-to-end interactions, as well interactions between the Tm and actin. Sequence alignment also revealed a short three amino acid motif of L-K-L (residues 11-13) present in each of the Tms except Cdc8. Although only half of this motif is predicted to lie within the overlap region, modelling predicted replacing the alanine at position 11 with a leucine residue (within the overlap) would fill a hydrophobic pocket present in the wild type dimer (Figure 1D). We were therefore intrigued to explore whether this divergence in amino terminal Tm sequence could play a role in modulating end-to-end interactions within the Cdc8 polymer.

A series of Cdc8 amino-terminal mutants were therefore generated in which either single acidic residues had been replaced (Cdc8-D2A, Cdc8-E6A, Cdc8-E6K & Cdc8-D16A) or the Ala-Arg-Ala residues at positions 11-13 had been replaced with the Leu-Lys-Leu motif, which is conserved in other Tm molecules (Cdc8-LKL). Each mutant protein was purified in a non-acetylated state from *E. coli*. For comparison wild type Cdc8 was purified in both acetylated and unacetylated forms from *S. pombe* and *E. coli* respectively. Each Cdc8 protein was subjected to SDS-PAGE (Figure 1E), electron spray mass-spectroscopy and spectrophotometric analyses to determine purity and concentration. The relative molecular mass of each full-length protein was as predicted, except for the D2A mutant, in which the amino-terminal methionine had been cleaved within the bacterial cell. This protein was subsequently named Cdc8-D2A* to highlight this amino terminal cleavage. To facilitate functional analyses of each mutant protein, each mutant gene was expressed within the fission yeast cell from the pREP41 expression vector and while none were found to have a dominant negative effect up the growth of the *S. pombe* cell (data not shown), only the *cdc8-D2A* gene was unable to complement the temperature sensitive growth defect of *cdc8-110* cells while

cells expressing *cdc8-D16A* displayed reduced growth (Figure 1F).

Circular dichroism (CD) analyses were performed upon each protein to assess the impact the amino acid substitutions had on the thermal stability of the dimer. The broad negative CD spectra peaks at 208 nm and 222nm consistent for α-helical structures were observed for the Cdc8 protein (Figure 2A). Spectra were equivalent for all Cdc8 proteins (not shown), and raw data curves for absorbance at 222 nm of three Cdc8 proteins highlighting the most dramatic effects are shown in Figure 2B. Figure 2C illustrates the first derivative plots for these data, from which midpoint melting temperatures (T_m) were calculated (Table 2). Acetylation of the wild type Cdc8 protein had a minimal effect upon the thermal stability of the Cdc8 dimer, increasing the T_m only slightly from 34.7ºC to 35.4ºC (Table 2). For Cdc8-D2A* a significant decrease in thermal stability was observed, with the T_m for this protein equal to 32.4ºC, which is likely to be more of a reflection of the lack of methionine 1 than loss of charge at the second residue. The E6A mutation had little effect on thermal stability, when compared to the WT protein, with a T_m of 34.4ºC. The E6K mutation increased thermal stability to equal that of the wild-type acetylated Cdc8, 35.4ºC and the D16A mutation increased the T_m slightly further to 35.9ºC. However, a dramatic increase in thermal stability was observed for the Cdc8-LKL protein (T_m = 37.3ºC). These data confirm that as predicted (apart from the cleaved D2A), none of the amino terminal mutations had a detrimental effect on Cdc8 dimer stability.

End-to-end interactions between the amino and carboxyl termini of Cdc8 dimers allow the protein to polymerise. Viscometry was used to investigate the effect amino terminal mutations had upon the ability of Cdc8 to form filaments. In this assay a higher viscosity correlates with a greater capacity to form filaments. Figure 3A shows viscosity data for four Cdc8 proteins emphasizing the most dramatic effects, while a summary of viscosity for each of the Cdc8 proteins in the absence of NaCl is presented in Table 1. In the absence of NaCl Cdc8 has a viscosity of 1.08 centistokes (cSt). Acetlyation of Cdc8 had a significant effect increasing viscosity to 1.15 cSt. In contrast the Cdc8-D2A* protein was unable to form any detectable end-to-end interactions, as the viscosity of 1.05 this protein was equal to the buffer control containing no protein. The E6A, E6K and D16A mutations increased the viscosity to a value comparable with that of Cdc8-ACE, the recorded values were 1.13 cSt, 1.15 cSt and 1.14 cSt respectively. The most striking effect was observed with Cdc8-LKL, which had an increased viscosity of 1.22 cSt. In addition the viscosity of Cdc8-LKL in the presence of 200 mM NaCl was still greater than the buffer control. At this salt concentration the viscosity of each of the other samples was equal to that of the buffer. These data suggest that each amino terminal mutation had a significant impact upon end-to-end interactions between the Cdc8 dimers, and that the D2A, E6A, E6K and D16A effects are electrostatically driven whereas the LKL mutant effects are more likely a hydrophobic effect.

Electron microscopy of rotary shadowed Tm was used to directly observe and compare the lengths of unacetylated Cdc8, Cdc8-ACE and Cdc8-LKL polymers in low salt conditions (5 mM). Figure 3B shows electron micrographs representative of what was typically observed for each protein. Non-acetylated Cdc8 protein was observed mainly as a population of single dimers and occasionally filaments of 2 interacting dimers, whereas the

acetylated Cdc8 protein was seen as distinctly longer filaments, made up of two to four dimers (Figure 3C). Consistent with its high viscosity the Cdc8-LKL protein was capable of forming longer filaments, with a longer average length (Figure 3C). These observations were consistent with the viscosity data and gave confidence that the mutant proteins (except Cdc8-D2A*) form longer filaments than the unacetylated wild type protein.

From these images we were also able to determine the persistence length for each protein. The persistence length of unacetylated Cdc8 was calculated as 50 nm, which is approximately twice the length of a single Cdc8 dimer (24 nm). The persistence length of Cdc8-LKL was equal (90 nm, ≈ 4 dimers) to that of the acetylated protein. Therefore although the Cdc8-LKL protein is capable of forming longer filaments than the acetylated Cdc8 protein it does not stiffen the protein or inter-dimer interactions.

In addition to effects on Cdc8 stability and end-to-end contacts we wished to explore the effects of these mutations on other protein–protein interactions, specifically the interaction with actin. To do this we initially performed co-sedimentations experiments to determine the affinity of each protein for actin. Examples of SDS-PAGE gels used to determine binding affinity of three Cdc8 mutants are presented in Figure 4. In Figures 4A and 4B the top bands are actin and the density remain approximately constant. The bottom bands are Cdc8 protein and the density increases as Cdc8 dimer concentrations increase from left to right. Figure 4A is an example of a Cdc8 mutant binding weakly to actin. Even at 20 μM Cdc8, only a small proportion of the protein is observed in the pellet fraction, while a large amount of Cdc8 remains in the supernatant. Conversely Figure 4B shows an example of a Cdc8 mutant which binds strongly to actin. A faint band can be observed in the pellet with as little as 0.2 μM Cdc8, a much denser band is visible at 8 μM Cdc8. Less Cdc8 can be observed in the supernatant at equivalent Tm concentrations. Typical binding curves for WT and Cdc8 mutants are presented in Figure 4D. Unacetylated Cdc8 has a $K_{50\%}$ of 2.76 μM, the acetylated protein has an increased affinity for actin with a $K_{50\%}$ of 0.46 μM. These observations for WT unacetylated and acetylated Tms were consistent with previously published data [15].

The truncated Cdc8-D2A* protein bound extremely weakly to actin and a binding curve could not be generated as the binding coefficient was estimated to be greater than 20 μM. The effect of the E6A and E6K mutations was to increase the affinity of these mutant proteins for actin, with values for $K_{50\%}$ of 0.32 μM and 0.45 μM respectively. These values are comparable with the WT acetylated protein. The $K_{50\%}$ for Cdc8-D16A is 2.27, and although lower, statistical analysis indicate no significant difference from the unacetylated wild type protein. This was expected as it is consistent with the mutation having no effect upon the Tm overlap region and also having minimal impact upon the interaction of the Tm dimer with actin. Surprisingly the Cdc8-LKL protein was observed in the pellet in the absence of actin (Figure 4C). As a result of this a binding curve could not be generated. Several attempts to determine a value using high salt conditions and lower centrifugation speeds were also unsuccessful and it was not possible to determine the actin affinity of this protein using this method. This is potentially either a consequence of an alteration to the overlap region or a change in shape of the Cdc8-LKL filament. Each $K_{50\%}$ was determined as an average

from at least 3 independent experiments. Averages and standard deviations for WT and Cdc8 mutants were calculated and are summarised in Table 2.

Both unmodified and acetylated Cdc8 have been shown to be capable of regulating the interaction between myosins and actin [15], with the modified protein doing so significantly more effectively and this modification is necessary for the regulation of myosin II activity [16, 22, 23]. We therefore decided to use an ATPase assay to investigate the influence of Cdc8 amino terminal mutations on regulation of myosin ATPase activity, as this provides a measure of how the altered Cdc8 protein affects interactions outside of the Tm polymer. Figure 5A shows ADP release at increasing concentrations of S1 for WT and Cdc8 mutants. The rates of ADP release per micromole of S1 were expressed as a fraction of the maximal rate observed for actin and S1 in the absence of Tm protein (Table 2). Consistent with previous *in vivo* and *in vitro* studies [15, 16, 22] both unacetylated and acetylated Cdc8 reduced the rate of actin activated ATPase activity of rabbit skeletal S1 to 0.46 and 0.17 of maximal.

When Cdc8-E6A or Cdc8-E6K were bound to actin, ATPase rates were reduced to 0.14 and 0.15 of maximal respectively, comparable to those observed for acetylated Cdc8. The Cdc8-D2A protein was not assayed owing to its extremely low affinity for actin. Cdc8-LKL had only a small inhibitory effect on S1 ATPase rate, reducing it to only 0.90 of maximal, however as an inhibitory effect was observed the affinity of Cdc8-LKL for actin was determined using this assay. ATPase rates were recorded in the presence of increasing Cdc8-LKL concentrations and a $K_{50\%}$ value of 5.2 μM calculated as the Cdc8-LKL concentration producing half of maximum inhibition. As a control the same method was used to calculate the $K_{50\%}$ of $Cdc8^{ACE}$. A value of 0.41 μM was determined, comparable to the value obtained using cosedimentation.

DISCUSSION

We have generated novel Cdc8 amino terminal mutants that were predicted to disrupt protein-protein interactions without adversely affecting the integrity of the Cdc8 dimer. A model of the Cdc8 overlap region was generated, based upon the structure of mammalian muscle Tm, not the yeast protein, and while each of the Tm overlap structures determined to date are based upon artificial constructs, they were predicted to mimic the endogenous structure [4, 6, 24].

The Cdc8 model predicted that none of the mutations generated in this study would have an adverse effect on Cdc8 dimer formation (Figure 1C). This is consistent with the prediction that the major effect amino-terminal acetylation has upon Tm is to stabilise the α-helical conformation at the amino terminus through the formation of intra-helical hydrogen bond to the amide hydrogen of the conserved hydrophobic residue in position 4 [3, 4]. The T_m of Cdc8 was increased by less than a degree when the protein was acetylated, however the enthalpy of unfolding rose by 27 kJ mol^{-1}. This 15.8% change in enthalpy indicates that acetylation affects the stability of a large proportion of the protein, significantly more than the predicted overlap region alone. Comparison between modelled structures of the wild type and LKL mutant proteins suggest the side chains of leucine 11 in the mutant protein fills a hydrophobic pocket present in the wild type (Figure 1D), which is likely to have a significant positive effect upon the stability of the overlap region.

Consistent with this the Cdc8-LKL protein had an 18.6% increase in enthalpy over the unacetylated protein, which corresponds to a stabilising effect on an even larger proportion of the dimer than the acetylated wild type protein.

The propensity of Cdc8 to form filaments as measured by viscosity was affected by amino terminal modifications. Acetylation of Cdc8 increased its viscosity significantly when compared to the unacetylated protein. This is consistent with the stabilising effect acetylation is predicted to have on the amino terminal α-helix, through the formation of intra-helical hydrogen bonds with the conserved hydrophobic residue four amino acids away [4]. Interestingly the E6A, E6K and D16A mutations increased the viscosity of these unacetylated proteins to values comparable to acetylated Cdc8. The predicted distances between mutated residues and charged residues on adjacent carboxy termini strands of the overlapping region are too great (> 12 Å) to form inter-chain electrostatic interactions. Interestingly, while there are 4 positive and 5 negatively charged residues on the Cdc8 amino terminus, there are only 5 negative charges on the carboxyl terminus (Figure 1C). Therefore changes in inter-chain interactions caused by mutating residues D2, E6 or D16 are likely to be due to changes in the overall electrostatic interactions between the regions. However each of these single mutations are likely to affect the stabilization of the amino-terminal helix. Indeed it has been predicted that the amino terminus of muscle Tm is stabilized by interactions between lysine 6 and acetylated methionine 1 [11]. This is consistent with the results presented here for the Cdc8-E6K mutation, which would mimic the stabilizing amino-terminal intra-helical electrostatic interactions observed in vertebrate muscle Tms. It is therefore likely that the observed differences were due to stabilisation of the amino terminal coil structure (through the formation of intra-helical hydrogen bonds) and changes in the overall charge of the amino terminus.

Perhaps unsurprisingly, the LKL mutation had the most dramatically effect upon viscosity illustrating this protein was capable of forming still longer polymers, which is consistent with the molecular models which indicate the A11L mutation is likely to have a significant effect upon the stability of the amino-terminal helical structure. The EM data also indicated that acetylation and the LKL mutation stiffened the Cdc8 protein, as reflected by an increased persistence length when compared to unacetylated Cdc8.

The ability of Cdc8 to form filaments was largely reflected in the ability of Cdc8 to bind to actin. The D2A protein, of which the amino terminal methionine had been cleaved by the *E. coli* expression system, was unable to form filaments (Figure 3A) and subsequently unable bind actin, consistent with the cooperative binding model [10] of Tm binding to actin. The unacetylated E6A and E6K mutants which were able to form filaments as readily as $Cdc8^{ACE}$ correspondingly had an affinity for actin comparable to the acetylated protein. Interestingly the D16A mutant, also able to form filaments as readily as $Cdc8^{ACE}$, did not show a comparable increase in actin affinity. This increase in propensity to form filaments suggests the ability to form filaments can be affected by more than the Tm overlap region, as predicted.

Surprisingly the LKL mutant was found to have a weak affinity for actin. It is unlikely mutation of alanine 13 in the *f* position of the heptad to an evolutionarily conserved leucine would inhibit interactions between Tm and actin. Tm dimers are thought to have a natural curvature that facilitates their

binding to actin [25, 26]. This reduction in actin affinity may therefore be due to the mutation changing the shape of the Tm polymer. Alternatively the propensity of the Cdc8-LKL to form longer filaments (consistent with the viscometry and EM data, together with its ability to sediment in the absence of actin, and the modeling) may inhibit its interaction with the actin polymer. This is consistent with a cooperative model of Tm binding [10], in which the overall shape of the Tm dimer is important for actin binding and that inherent helical contour of Tm dimer are an essential feature that facilitates the binding of the elongated protein on actin.

Acetylated Cdc8 binding to actin was able to inhibit the actin induced ATPase activity of myosin sub-fragment 1 (S1), and is consistent with reported findings that Cdc8 reduced fission yeast Myo2-driven actin filament gliding in motility assays [22]. The unacetylated Cdc8, which has weaker end-to-end interactions, lower affinity for actin (Figures 3A and 4D) and a higher occupancy of the 'open' position on actin [15], had a correspondingly reduced inhibitory effect on S1 ATPase rate (table 2). The inhibition of S1 ATPase rate by Cdc8-E6A, Cdc8-E6K and D16A reflected their affinity for actin. The E6A and E6K proteins, which had an affinity for actin comparable to the acetylated protein (Figure 4D), were found to inhibit ATPase rate correspondingly (Table 2). Where as the Cdc8-D16A protein, which had a lower affinity for actin, correspondingly had less of an inhibitory effect on ATPase activity.

In contrast the Cdc8-LKL protein only weakly inhibited S1 ATPase rate (table 2). Different Tms occupy different positions on actin filaments [27, 28] and changes in one part of the molecule appear to have significant effects further along. One hypothesis is that the substitution of 3 amino acids (ARA to LKL) alters the molecule in such a way that it occupies a more 'open' position on the actin filament, and as a result is less able to inhibit myosin ATPase rate. The small changes to the charge and/or size of residues within the amino terminus dramatically altered the biochemical properties of the proteins *in vitro,* however, with one exception, each mutant protein (Cdc8-D2A*) was capable of complementing the function of the temperature sensitive *cdc8-110* allele within *S. pombe*. However, it has yet to be assessed whether the amino terminal residue is cleaved from the Cdc8-D2A protein within the yeast cell.

Why is the conserved LKL motif replaced with ARA residues in *S. pombe* Cdc8? This replacement is conserved, and there are only minor differences in lengths of residue side chains, but this replacement has a surprising dramatic effect on the protein's ability to polymerise *in vitro*. Molecular modelling predicts the A11L mutation would fill a hydrophobic pocket present in the wild type Cdc8 overlap region, and therefore stabilises the overlap of Tm dimers. Potentially the ARA residues allow acetylation to regulate the protein more than would otherwise be possible if Cdc8 were to possess the LKL motif. Unlike other yeast and metazoan cells, *S. pombe* expresses a single Tm isoform. Therefore the ability to modulate the physical properties of this sole Tm is likely to be crucial for the growth and viability of the fission yeast

REFERENCES

1 Urbancikova, M. and Hitchcock-DeGregori, S. E. (1994) Requirement of amino-terminal modification for striated muscle alpha-tropomyosin function. J Biol Chem **269**, 24310-24315

2 Coulton, A., Lehrer, S. S. and Geeves, M. A. (2006) Functional homodimers and heterodimers of recombinant smooth muscle tropomyosin. Biochemistry **45**, 12853-12858

3 Brown, J. H., Kim, K. H., Jun, G., Greenfield, N. J., Dominguez, R., Volkmann, N., Hitchcock-DeGregori, S. E. and Cohen, C. (2001) Deciphering the design of the tropomyosin molecule. Proc Natl Acad Sci U S A **98**, 8496-8501

4 Frye, J., Klenchin, V. A. and Rayment, I. (2010) Structure of the tropomyosin overlap complex from chicken smooth muscle: insight into the diversity of N-terminal recognition. Biochemistry **49**, 4908-4920

5 Greenfield, N. J., Stafford, W. F. and Hitchcock-DeGregori, S. E. (1994) The effect of N-terminal acetylation on the structure of an N-terminal tropomyosin peptide and alpha alpha-tropomyosin. Protein Sci **3**, 402-410

6 Greenfield, N. J., Huang, Y. J., Swapna, G. V., Bhattacharya, A., Rapp, B., Singh, A., Montelione, G. T. and Hitchcock-DeGregori, S. E. (2006) Solution NMR structure of the junction between tropomyosin molecules: implications for actin binding and regulation. J Mol Biol **364**, 80-96

7 Crick, F. (1953) The packing of [alpha]-helices: simple coiled-coils. Acta Crystallographica **6**, 689-697

8 Hitchcock-DeGregori, S. E., Song, Y. and Greenfield, N. J. (2002) Functions of tropomyosin's periodic repeats. Biochemistry **41**, 15036-15044

9 Hitchcock-DeGregori, S. E. and Varnell, T. A. (1990) Tropomyosin has discrete actin-binding sites with sevenfold and fourteenfold periodicities. J Mol Biol **214**, 885-896

10 Holmes, K. C. and Lehman, W. (2008) Gestalt-binding of tropomyosin to actin filaments. J Muscle Res Cell Motil **29**, 213-219

11 Hitchcock-DeGregori, S. E. and Heald, R. W. (1987) Altered actin and troponin binding of amino-terminal variants of chicken striated muscle alpha-tropomyosin expressed in Escherichia coli. J Biol Chem **262**, 9730-9735

12 Pittenger, M. F., Kistler, A. and Helfman, D. M. (1995) Alternatively spliced exons of the beta tropomyosin gene exhibit different affinities for F-actin and effects with nonmuscle caldesmon. J Cell Sci **108 (Pt 10)**, 3253-3265

13 Moraczewska, J., Nicholson-Flynn, K. and Hitchcock-DeGregori, S. E. (1999) The ends of tropomyosin are major determinants of actin affinity

and myosin subfragment 1-induced binding to F-actin in the open state. Biochemistry **38**, 15885-15892

14 Balasubramanian, M. K., Helfman, D. M. and Hemmingsen, S. M. (1992) A new tropomyosin essential for cytokinesis in the fission yeast S. pombe. Nature **360**, 84-87

15 Skoumpla, K., Coulton, A. T., Lehman, W., Geeves, M. A. and Mulvihill, D. P. (2007) Acetylation regulates tropomyosin function in the fission yeast *Schizosaccharomyces pombe*. J Cell Sci **120**, 1635-1645

16 Coulton, A. T., East, D. A., Galinska-Rakoczy, A., Lehman, W. and Mulvihill, D. P. (2010) The recruitment of acetylated and unacetylated tropomyosin to distinct actin polymers permits the discrete regulation of specific myosins in fission yeast. J Cell Sci **123**, 3235-3243

17 Moreno, S., Klar, A. and Nurse, P. (1991) Molecular genetic analysis of fission yeast Schizosaccharomyces pombe. Methods Enzymol **194**, 795-823

18 Sousa, D., Cammarato, A., Jang, K., Graceffa, P., Tobacman, L. S., Li, X. E. and Lehman, W. Electron microscopy and persistence length analysis of semi-rigid smooth muscle tropomyosin strands. Biophys J **99**, 862-868

19 Li, X. E., Holmes, K. C., Lehman, W., Jung, H. and Fischer, S. (2010) The shape and flexibility of tropomyosin coiled coils: implications for actin filament assembly and regulation. J Mol Biol **395**, 327-339

20 Li, X. E., Lehman, W. and Fischer, S. (2010) The relationship between curvature, flexibility and persistence length in the tropomyosin coiled-coil. J Struct Biol **170**, 313-318

21 Monteiro, P. B., Lataro, R. C., Ferro, J. A. and Reinach Fde, C. (1994) Functional alpha-tropomyosin produced in Escherichia coli. A dipeptide extension can substitute the amino-terminal acetyl group. J Biol Chem **269**, 10461-10466

22 Stark, B. C., Sladewski, T. E., Pollard, L. W. and Lord, M. (2010) Tropomyosin and myosin-II cellular levels promote actomyosin ring assembly in fission yeast. Mol Biol Cell **21**, 989-1000

23 Clayton, J. E., Sammons, M. R., Stark, B. C., Hodges, A. R. and Lord, M. (2010) Differential regulation of unconventional fission yeast myosins via the actin track. Curr Biol **20**, 1423-1431

24 Murakami, K., Stewart, M., Nozawa, K., Tomii, K., Kudou, N., Igarashi, N., Shirakihara, Y., Wakatsuki, S., Yasunaga, T. and Wakabayashi, T. (2008) Structural basis for tropomyosin overlap in thin (actin) filaments and the generation of a molecular swivel by troponin-T. Proc Natl Acad Sci U S A **105**, 7200-7205

25 Brown, J. H., Zhou, Z., Reshetnikova, L., Robinson, H., Yammani, R. D., Tobacman, L. S. and Cohen, C. (2005) Structure of the mid-region of

tropomyosin: bending and binding sites for actin. Proc Natl Acad Sci U S A **102**, 18878-18883

26 Lorenz, M., Poole, K. J., Popp, D., Rosenbaum, G. and Holmes, K. C. (1995) An atomic model of the unregulated thin filament obtained by X-ray fiber diffraction on oriented actin-tropomyosin gels. J Mol Biol **246**, 108-119

27 Lehman, W., Hatch, V., Korman, V., Rosol, M., Thomas, L., Maytum, R., Geeves, M. A., Van Eyk, J. E., Tobacman, L. S. and Craig, R. (2000) Tropomyosin and actin isoforms modulate the localization of tropomyosin strands on actin filaments. J Mol Biol **302**, 593-606

28 Pittenger, M. F., Kazzaz, J. A. and Helfman, D. M. (1994) Functional properties of non-muscle tropomyosin isoforms. Curr Opin Cell Biol **6**, 96-104

ACKNOWLEDGEMENTS

We thank Nancy Adamek and Sam Lynn for purified actin, as well as Ian Bruce, Mike Geeves, Kay Barr for support and Mike Geeves for comments on the manuscript.

FUNDING

This work was funded by grants from the EU FP6 (NACBO-CT-2004-500804), the BBSRC (BB/F011784/1), as well a Traveling Fellowship from the Company of Biologists. The EM work and analysis was supported by grants from the National Institutes of Health to W.L. (HL86655 and HL36153); D.S. was supported by an NIH training grant (HL007224) to the Whitaker Cardiovascular Institute at Boston University (J.E. Freedman, P.I.). Electron microscope facilities, supported by NIH grant (RR08426) to Roger Craig, at the University of Massachusetts Medical School were used.

Biochemical Journal Immediate Publication. Published on 09 Jun 2011 as manuscript BJ20101316

FIGURE LEGENDS

Figure 1. (A) Diagram illustrating the heptad repeats within two α-helices highlighting hydrophobic interactions between residues in the *a* and *d* positions as well as ionic interactions (dotted lines) between residues in *e* and *g* positions. (B) Sequence alignment of 20 amino terminal amino acid residues from fission yeast, budding yeast and mammalian tropomyosins, highlighting position in the heptad repeat (lower case), conserved residues (grey highlight) and positions of mutations introduced in this study (bold). (C) Model of the Cdc8 overlap complex displayed as ribbons (upper panel) or surface (lower panel) with the C termini in green, N termini in orange. The D2, E6, D16 residues and ARA motif are labelled in the ribbons form. The surface representation displays charges within the overlap region; Asp and Glu residues are highlighted in red; Arg and Lys in blue. (D) Surface representations of models of the wild type Cdc8 (upper panel) and LKL mutant (lower panel). Reside 11 (Ala in wild type and Leu in the mutant) is highlighted in pink - note that the mutant Leu side chain fills a hydrophobic pocket present in the wild type. (E) Coomassie stained SDS-PAGE gel showing purified WT and mutant Cdc8 proteins. (F) *cdc8-110* cells expressing WT and mutant *cdc8* alleles under the control of the *nmt41* promoter grown on EMM agar, lacking leucine and containing thiamine at 36^0C.

Figure 2. (A) Circular dichroism spectrum for unacetylated Cdc8. (B) Differential absorbance data for unacetylated Cdc8, Cdc8–D2A, and Cdc8–LKL at 222 nm. (C) First derivative plots for unacetylated Cdc8, Cdc8–D2A, and Cdc8–LKL at 222 nm

Figure 3. (A) Viscosity of 20 μM Cdc8 proteins and buffer control at increasing NaCl concentration (0 to 200 mM) at 23 ^{0}C. (B) Electron micrographs of rotary shadowed Cdc8, $Cdc8^{ACE}$ and Cdc8–LKL proteins. The longest typical particles for each sample are shown. (C) Polymer lengths of Cdc8, Cdc8ACE and Cdc8-LKL calculated from electron micrographs (n>200).

Figure 4. SDS-PAGE gels of the pellets and supernatants from co-sedimentation experiments of (A) Cdc8-D2A and (B) Cdc-E6K with actin over increasing tropomyosin concentrations in the presence of 100 mM KCl. (C) Cdc8-LKL pellets and supernatants in the absence of actin. (D) Binding curves of free Cdc8 concentration against ratio of density of actin, for WT and mutants Cdc8, measured by densitometry of co-sedimentation SDS-PAGE gels. Curves represent Hill equation lines of best fit.

Figure 5. (A) ATPase rate against S1 concentration for WT and mutant Cdc8 proteins. Dashed grey lines correspond to the minimum (S1) and maximum (S1+actin) rate controls, black lines represent rates in the presence of each Cdc8 protein. Actin concentration was 1 μM. Cdc8 dimer concentrations were 1 μM for $Cdc8^{ACE}$ and Cdc8-E6A and 2.5 μM for Cdc8. (B) Binding curves for Cdc8-LKL and $Cdc8^{ACE}$ calculated from ATPase measurements with 1 μM actin, 10 μM S1 and increasing concentrations of Cdc8. Curves represent Hill equation lines of best fit.

Table 1 – *Oligonucleotides used in this study*.

Lab Stock Number	Name	Sequence
197	cdc8D2AJC20F	5´ GAG ATA TAC ATA TGG CCA AGC TTA GAG AG 3´
198	cdc8D2AJC20R	5´ CTC TCT AAG CTT GGC CAT ATG TAT ATC TC 3´
199	cdc8E6AF	5´ GGA TAA GCT TAG AGC GAA AAT TAA TGC CG 3´
200	cdc8E6AR	5´ CGG CAT TAA TTT TCG CTC TAA GCT TAT CC 3´
201	cdc8D16AF	5´ CGT GCT GAG ACT GCA GAG GCT GTC GC 3´
202	cdc8D16AR	5´ GCG ACA GCC TCT GCA GTC TCA GCA CG 3´
232	cdc8LKLF	5´ GAG AAA ATT ATT GCC TTA AAA CTC GAG ACT GAT GAG GC 3´
233	cdc8LKLR	5´ GCC TCA TCA GTC TCG AGT TTT AAG GCA TTA ATT TTC TC 3´
258	cdc8E6KF	5´ GGA TAA GCT TAG AAA GAA AAT TAA TGC C 3´
259	cdc8E6KR	5´ GGC AAT AAT TTT CTT TCT AAG CTT ATC C 3´

Table 2 – *Summary of analysis of amino terminal Cdc8 mutant proteins*.

Tm protein	Source	Mass (Da) [1]	Tm (ºC)[2]	$K_{dimerisation}$ (nM)[2,3]	ΔH[2,4]	Kinematic Viscosity[2,5,6]	Persistence Length	$K_{50\%}$[2,7] (100mM KCl)	ATPase[2,8,9] activity	Normalised ATPase[10]	% Inhibition of ATPase	Relative growth in *cdc8-110* cells
Cdc8	*E. coli*	18,964	34.7	11.5 ± 2.9	144.73	1.07	50nm ± 10	2.76 ± 0.22	0.044 ± 0.002	1.00	54.9%	-
Cdc8 (*acetylated*)	*S. pombe*	19,006	35.4	1.3 ± 0.4	171.8	1.15	90nm ± 20	0.46 ± 0.10	0.017 ± 0.001	0.46	81.3%	1.00
Cdc8-D2A	*E. coli*	18,788	32.4	135 ± 29	128.3	1.05	-	> 20	-	-	-	0.00
Cdc8-E6A	*E. coli*	18,905	34.4	16.3 ± 4.1	143.47	1.13	-	0.32 ± 0.14	0.014 ± 0.003	0.18	87.4%	1.04
Cdc8-E6K	*E. coli*	18,963	35.4	19.5 ± 4.7	130.2	1.15	-	0.45 ± 0.10	0.015 ± 0.003	0.15	87.1%	1.22
Cdc8-D16A	*E. coli*	18,919	35.9	1.8 ± 0.5	159.8	1.14	-	2.27 ± 0.31	0.028 ± 0.001	0.29	77%	0.80
Cdc8-LKL	*E. coli*	19,020	37.3	0.19 ± 0.06	177.37	1.22	90nm ± 20	5.19 *	0.086 ± 0.008	0.90	6%	1.49

[1]Determined by electronspray MS; [2]Average of 3 experiments ; [3]$K_D$imerisation = [Monomer]^2/[Dimer] using Equation (2); [4]@ 25ºC; [5] Measured at [20µM] (centistokes); [6] Variance < 0.001; [7]using 10µM actin; [8]µmole Pi sec^{-1}µM S1^{-1}; [9]background S1 rate subtracted; [10]Normalised against rate with unacetylated Cdc8; * Determined from ATPase assays

Biochemical Journal Immediate Publication. Published on 09 Jun 2011 as manuscript BJ20101316

Figure 1

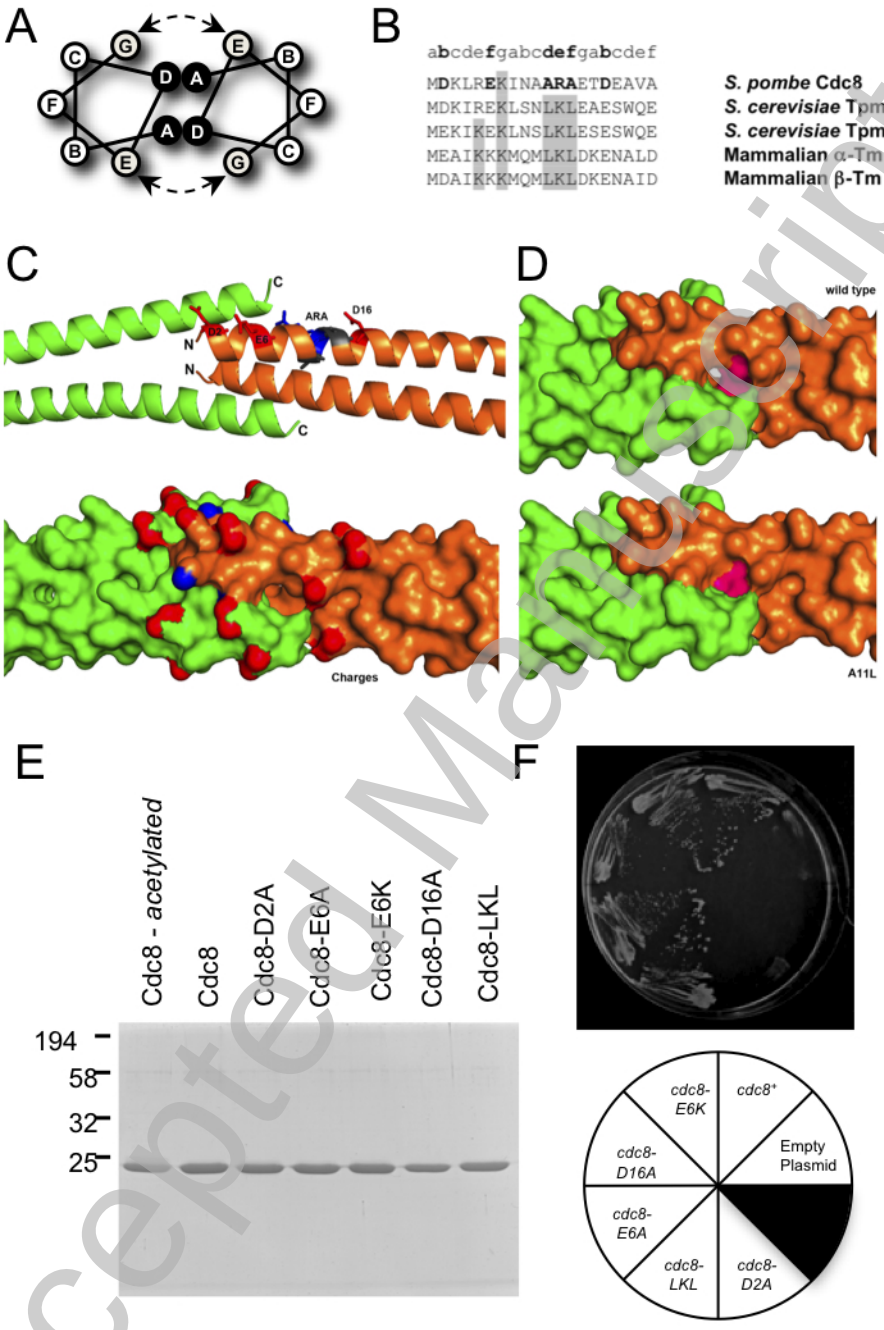

Figure 2

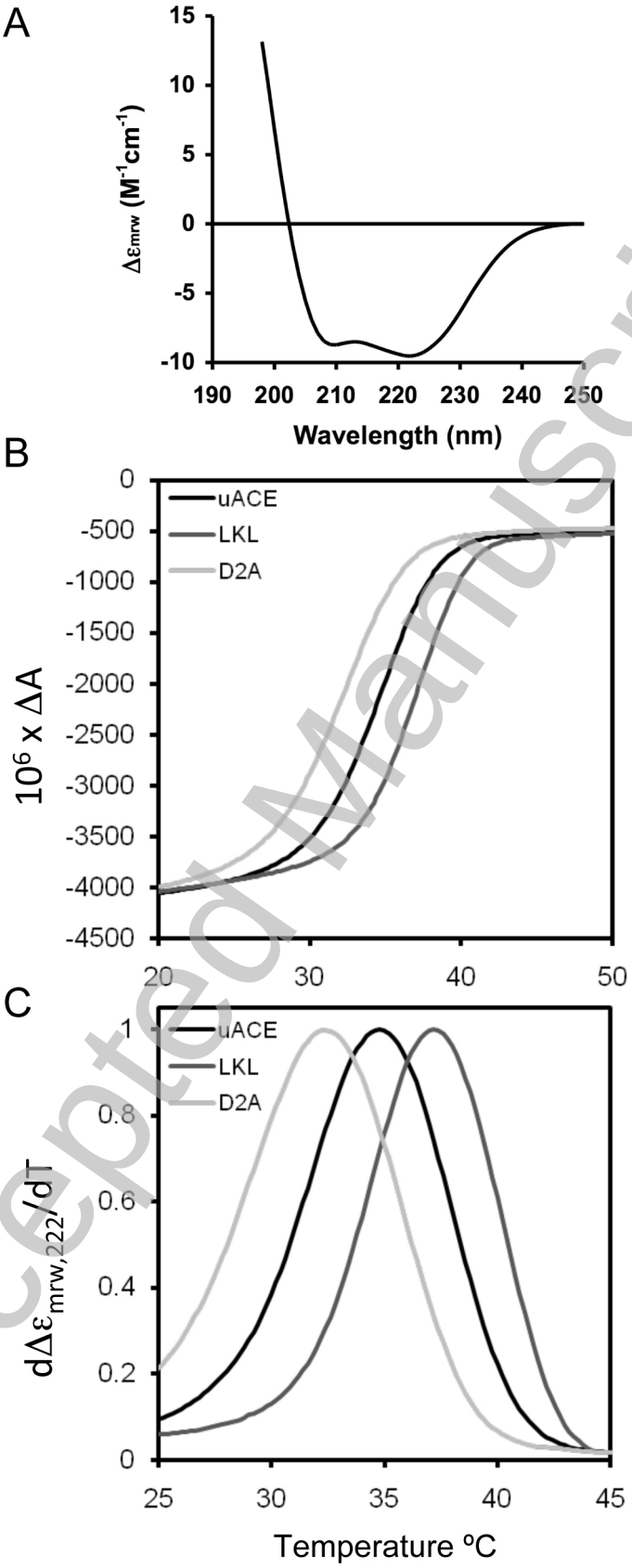

Figure 3

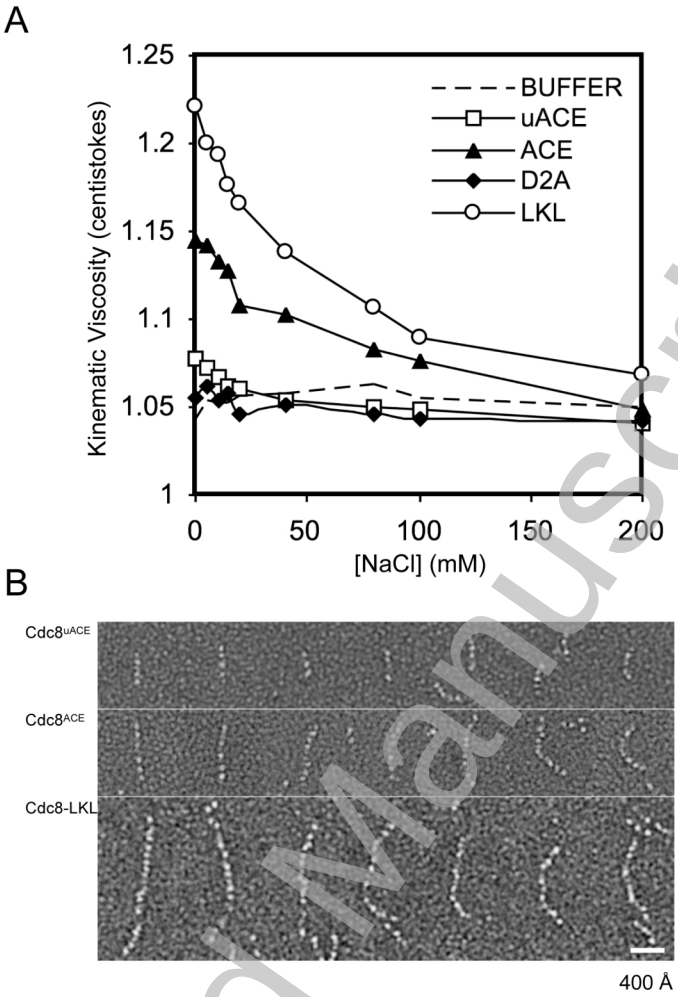

C

Protein	Single dimer	2 x dimer	3 x dimer	4 or more dimers
Cdc8	93.33%	6.67%	0	0
Cdc8 (*acetylated*)	74.05%	19.62%	5.70%	0.63%
Cdc8-LKL	62.94%	24.12%	7.06%	5.88%

Figure 4

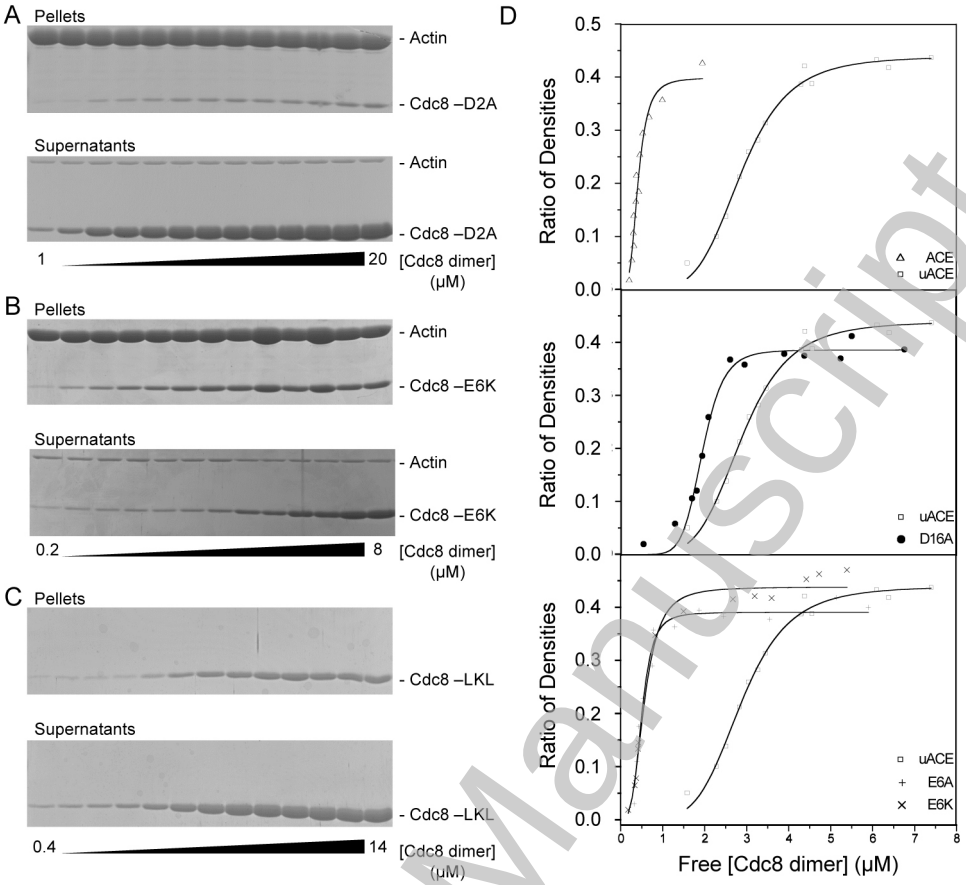

Figure 5